FLUID INDUCED INSTABILITY OF ROTOR SYSTEMS WITH JOURNAL BEARINGS

Jiří Tůma*, Jan Biloš**

The paper deals with stability of the rotor vibration in a journal bearing. The vibration signal, describing the rotor motion, is a complex signal. The real part of this kind of signals is a rotor displacement in the X-direction while the imaginary part is a displacement in the perpendicular direction, as we say in the Y-direction. A tool for analysis is a full spectrum, which results from the Fourier transform of the complex signal. The full multispectra of the rotor run up and coast down are employed to evaluate a magnitude as a function of the rotor rotation speed. The multispectrum slices serve to verification of the simplified mathematical model of a rotor system and to analyze the rotor vibration using a procedure based on the Nyquist stability criterion. As it is well known the self-excited vibration, called fluid induced vibration, occurs when the rotor rotation speed crosses a certain threshold.

Key words: *rotor system, journal bearings, full spectrum, fluid induced instability, self-exited vibration, mathematical model, stability margin*

1. Introduction

Full spectrum plots have recently received a great importance in diagnostics of rotors and journal bearings thanks to research work that was done at Bently Rotor Dynamics Research Corporation and Bently Nevada Corporation. Related work done in Korea and the People's Republic of China must be mentioned [1, 2].

The first research work dealing with the stability of the rotor vibration in journal bearings was published by Newkirk in 1924 as it is mentioned by Tondl in his book [3] published in 1965. The problem of the fluid-induced vibration was investigated by Muszynska and Bently at Bently Rotor Dynamics Research Corporation [4, 5]. One of the latest review of the work, which was done in this branch of science, is a paper published by Ecker and Tondl [6]. The topic of the mentioned paper is focused at solving the problem how to prevent the onset of the instability by control the bearing mount stiffness while increasing the rotor rotational speed. Their approach is based on the numerical solution of motion equations and establishing stability margins. The goal of the submited paper is drawing attention to the methods used in the control theory.

The first part of this paper discusses the benefits of full spectra and describes how to use full spectrum plots for analysing fluid-induced instabilities in a machinery diagnostic. The second part is focused at the relationship of the experimental data and the simplified lumped

* prof. Ing. J. Tůma, CSc., VSB – Technical University of Ostrava, Faculty of Mechanical Engineering, Department of Control Systems and Instrumentation, 17. listopadu 15 CZ-708 33 Ostrava, Czech Republic

** J. Biloš, Technical University of Ostrava, Faculty of Mechanical Engineering, Department of Mechanics, 17. listopadu 15 CZ-708 33 Ostrava, Czech Republic

parameter model of a rotor system. The control theory for closed-loop control systems is applied to the analysis of the mechanical system stability.

2. Orbit and full spectrum theory

In contrast to the frequency spectrum of a real time signal the full spectrum is a tool for processing complex signals. The real time signal gives information about position of a point along an axis while the complex signal describes the position of a point in a plane, which is called the complex plane. A complex number can be viewed as a point or a position vector on a two-dimensional Cartesian coordinate system. The topic of this paper is focused at the motion of rotors in journal bearings. The measurement instrumentation is shown in figure 1. The proximity probes are a non-contacting device, which measures the displacement motion and position of an observed rotor surface relative to the probe mounting location. Typically, proximity probes used for rotating machinery measurements operate on the eddy current principle, and measure rotor displacement motion and position relative to the machine bearings or housing. In addition to the rotor displacements, a voltage pulse for each turn of the rotor, called the Keyphasor® signal is used primarily to measure rotor rotation speed and serves as a reference for measuring vibration phase lag angle. It is an essential element in measuring rotor slow roll bow or runout information.

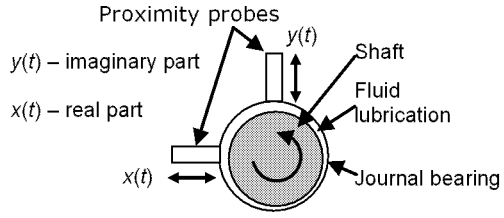

Fig.1: Instrumentation arrangement

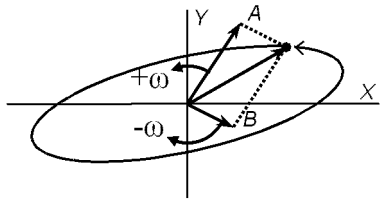

Fig.2: Model of orbit construction

The real signal, describing position of a point along for example the X-axis, can be constructed in a complex plane as a sum of two complex conjugate numbers or position vectors, A and B, rotating in opposite direction at the same frequency ω. The complex conjugate property means that the mentioned vectors are of the same length and their initial phases are opposite. The resulting signal is a real harmonic signal (sine or cosine function of time). If these vectors are not complex conjugate, then their sum as a function of time forms an ellipse in the complex plane, called an elementary orbit. The principle of the orbit construction is shown in figure 2. More than one pair of rotating position vectors at the different frequencies result in the more complicated planar motion than the elementary orbit. A tool for the decomposition of planar motion into the elementary orbits is the Fourier transform.

The real part of the mentioned position vector sum is a time signal $x(t)$, which describes displacement of the journal centre relative to the sleeve center-line in direction of the real axis, while the imaginary part is a time signal $y(t)$, which describes displacement in direction of the imaginary axis. The position vector end point is a complex function $x(t) + \mathrm{j}\, y(t)$ of time, where $\mathrm{j} = \sqrt{-1}$ is the imaginary unity.

It is well known that the Fourier transform of the real signal is a complex conjugate symmetric function of the frequency ω along $\omega = 0$. This is a reason that the frequency spectrum is plotted only for the positive value of the frequency. If the time domain signal

is a complex signal then the frequency domain function is non-symmetric and the plot of the magnitude of the complex numbers against the frequency is called a full spectrum. This spectrum contains both the positive and negative frequencies.

3. Orbit and full spectrum measurements

To study motion of the rotor in a journal bearing the RK 4 Rotor Kit device, product of Bently Nevada, was used. The proximity probes and the Keyphasor sensor belong to the instrumentation of Rotor Kit (see figure 3). The rotor centre-line motion can be analyzed only in the plane that is perpendicular to the rotor axis. The rotor rotates in the positive direction with respect to the placement of the proximity probes and their output signal polarity.

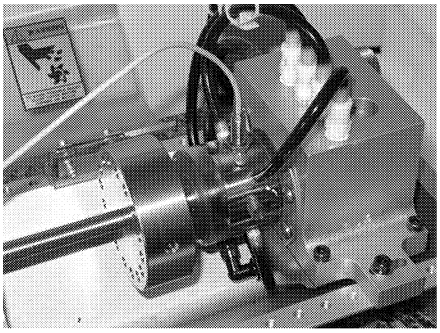

Fig.3: Bently Nevada Rotor Kit

The RPM profile determines the rotor operation condition. The run-up to the maximum of 2400 RPM is the first stage of the test. Then the test is continuing after a delay to the second stage that is a coast-down. The maximum value of RPM is below the first critical harmonic speed of the rotor. The RPM as a time function is shown in figure 4. The time history of the journal displacement in direction X, which is shown in figure 5, demonstrates that self-excited vibrations occur when the rotor rotation speed increases and reaches the certain value of RPM. These vibrations start to decay when the rotor rotation speed decreases and reaches the other value of RPM, which is less than the RPM value for the rotor run-up. It can be noted that the vibration decaying is slower and therefore it takes longer than the self-excited vibration startup.

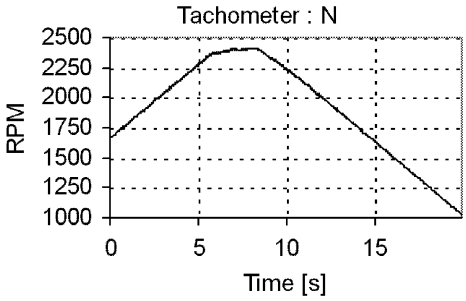

Fig.4: RPM time history

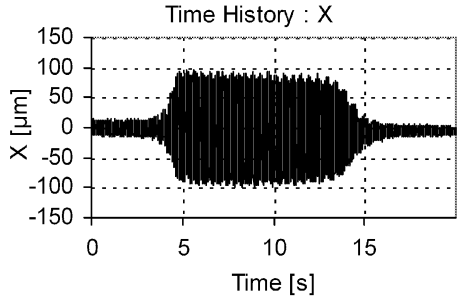

Fig.5: X-axis displacement time history

To determine the relationship between the journal centre vibration frequency and the rotor rotation speed, the frequency analysis of the journal centre vibration is performed. A full multispectrum of the signal $x(t)+\mathrm{j}\,y(t)$, which is composed from full spectra for RPM as the third axis, is shown in figure 6. This form of the 3D multispectrum is designated as a waterfall plot. The multispectrum frequency axis is in Hz. The orders 1 and 2 of rotational frequency form a line of individual spectrum peaks with frequency, which is determined by the instantaneous RPM. The spectrum component with the frequency of the 1 ord is called as a synchronous component.

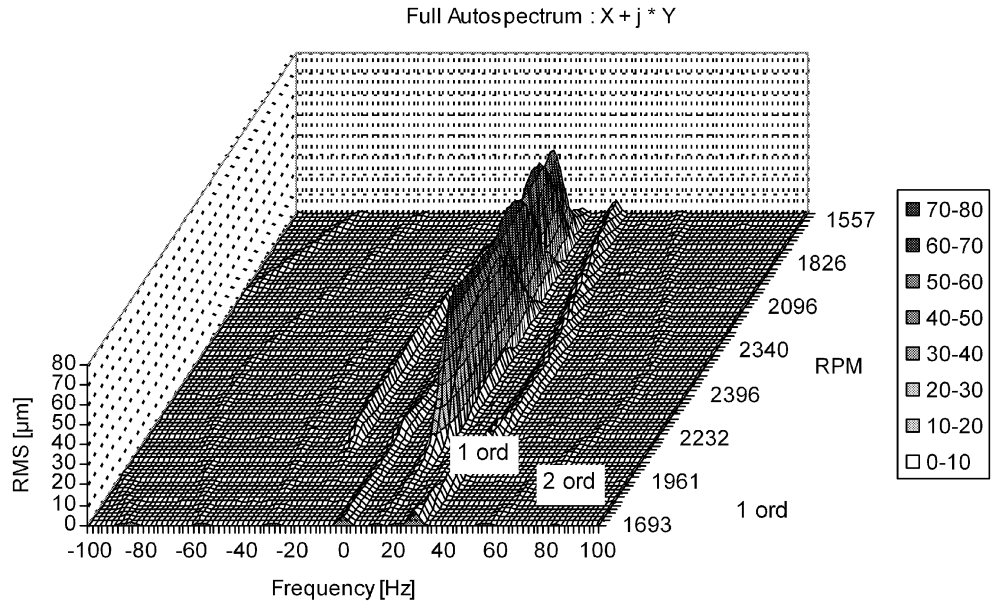

Fig.6: Full multispectrum of signal $x(t) + \mathrm{j}\, y(t)$ in Hz

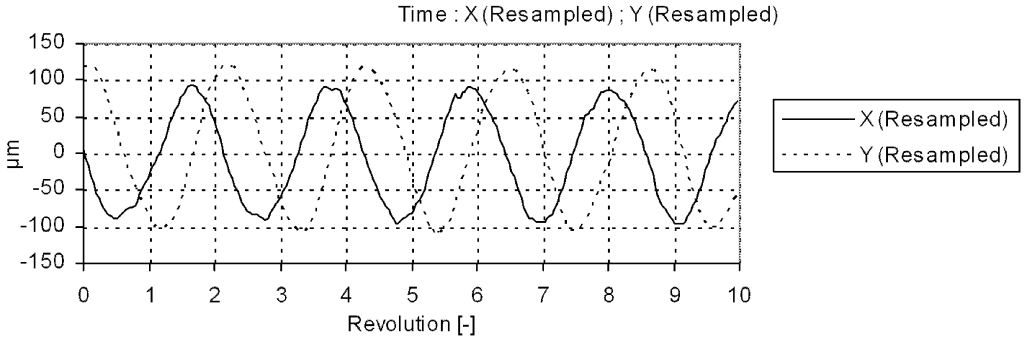

Fig.7: Displacement $x(t)$ and $y(t)$ during 10 revolutions at 2400 RPM beginning at 6.78 s

The analysis in the term of revolutions and orders gives better and clearer information about the rotor behavior than the analysis in term of time or frequency in Hz. After resampling both the signals $x(t)$ and $y(t)$ to the sampling frequency, which is proportional to the rotational frequency, the rotor displacement in the both directions is a function of revolution. The real and imaginary part of the complex resampled signal is shown in figure 7. 10 revolutions of the rotor correspond to less than 5 runs, called precession, along the elementary orbit. The shapes of the orbit for the different values of RPM are shown in figure 8 and 9.

The frequency of the dominating component in the overlaid full multispectra in figure 10 is equal to 0.475 ord. This subharmonic component in relation to the rotor rotational frequency is corresponding to rotor precession. As the frequency of the dominating component is positive what means that the sum of the position vectors, A and B (see figure 2) depend mainly on the position vector A, the precession is forward. The waterfall plot of the multispectrum with the frequency axis in order is shown in figure 11. As the peaks of

the subharmonic component lie on a straight line, which is parallel to the RPM axis, the frequency in order of the excited vibration is independent on the rotor rotational speed.

The magnitude of vibrations at the frequency of the 1 ord is ten times greater than the magnitude of vibrations at the frequency of the 2 ord. The synchronous component is a response to the natural unbalance of the rotor. The second and higher harmonics of the rotor rotational frequency generally result from a misalignment of the rotor and driving motor but this phenomenon is insignificant for the rotor under test.

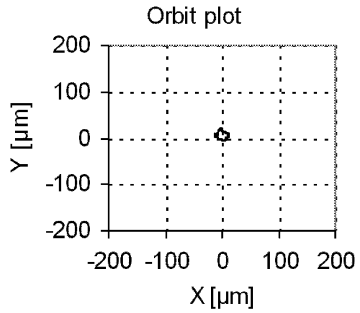

Fig.8: Orbit plot beginning at 0 s

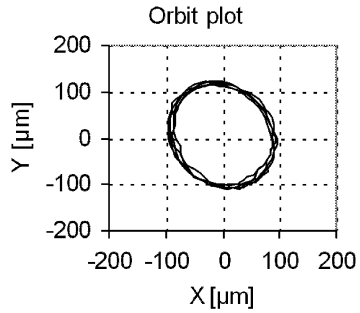

Fig.9: Orbit plot beginning at 6.78 s

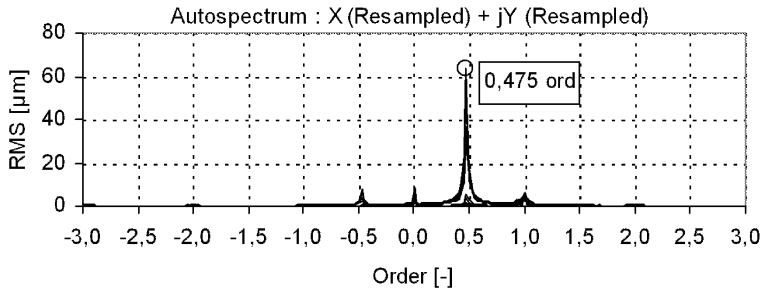

Fig.10: Full multispectrum of signal $x(t) + \mathrm{j}\, y(t)$ in orders

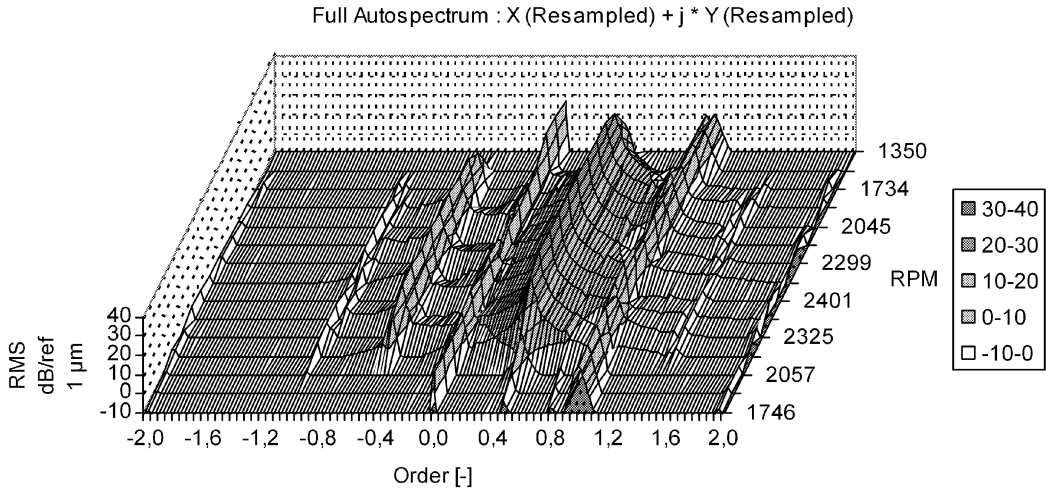

Fig.11: Full multispectrum of signal $x(t) + \mathrm{j}\, y(t)$ in order as a waterfall plot

4. Lumped parameter model of the rotor system

There are many ways how to model a rotor system, but this paper prefers an aproach, which is based on the concept developed by Muszynska [4] and Bently Rotor Dynamics Research Corporation [5]. The reason for this is that this concept offers an effective way to understanding the rotor instability problem. However, this simple mathematical model is inapplicable for solving practical technological problems. Another approach can be based on the lubricant flow prediction using a FE method for Reynolds equation solution, see [9] for instance. This approach does not allow to benefit of the dynamic system stability theory.

Let the rotor angular velocity is designated by Ω. It is assumed that the stator is fixed while rotor is rotating at the mentioned angular velocity. This paper proposes to use complex variables to describe motion of a rotor. The position of the journal centre in the complex plane, which origin is situated in the bearing centre, is designated by a position vector $\mathbf{r}$.

The internal spring, damping and tangential forces are acting on the rotor. The external forces refer to forces that are applied to the rotor, such as unbalance, impacts and preloads in the form of constant radial forces. All these external forces are considered as an input for the mathematical model based on the mentioned concept [7]. The identical solution was published by Tondl [8]. All these mentioned analyses are based on the same formula for evaluation of the bearing forces.

The fluid pressure wedge is the actual source of the fluid film stiffness in a journal bearing and maintains the rotor in equilibrium. These bearing forces can be modeled as a rotating spring and damper system at the angular velocity $\lambda\,\Omega$, where λ is a parameter, which is slightly less than 0.5. The parameter λ is denominated by Muszynska [4] as the fluid averaged circumferential velocity ratio. It is assumed that the rotating journal drags the fluid in a space between two cylinders into motion and acts as a pump. It is easy to understand that the fluid circular velocity is varying across the gap as a consequence of the fluid viscosity: At the surface of the journal, the fluid circular velocity is the same as the journal circumferential velocity and at the surface of the of the bearing, the fluid circular velocity is zero. The angular velocity $\lambda\,\Omega$ can be considered as the average angular velocity of the fluid but this quantity is only a fictive value. In fact, the angular velocity of the mentioned spring and damper system can be determined.

Fluid forces acting on the rotor in coordinates rotating at the same angular frequency as the spring and damper system are given by the formula

$$\mathbf{F}_{\mathrm{rot}} = K\,\mathbf{r}_{\mathrm{rot}} + D\,\dot{\mathbf{r}}_{\mathrm{rot}}\ , \tag{1}$$

where the parameters, K and D, are specifying proportionality of stiffness and damping to the journal centre displacement vector $\mathbf{r}_{\mathrm{rot}}$ and velocity vector $\dot{\mathbf{r}}_{\mathrm{rot}}$, respectively. The spring force acts opposite to the displacement vector. Assuming constant values of K and D (isotropic rotor system) and independence of these parameters on the journal eccentricity, the system is considered to be linear.

To model the rotor system, the fluid forces have to be expressed in the stationary coordinate system, in which the journal centre displacement and velocity vectors are designated by $\mathbf{r}$ and $\dot{\mathbf{r}}$, respectively. Conversion of the complex rotating vector $\mathbf{r}_{\mathrm{rot}}$ to the stationary coordinate system can be done by multiplication of this vector by $\exp(\mathrm{j}\,\lambda\,\Omega\,t)$, which is the same as multiplying the vector in the stationary coordinates by $\exp(-\mathrm{j}\,\lambda\,\Omega\,t)$, see figure 12. The relationship between the mentioned vectors in rotating and stationary coordinates are

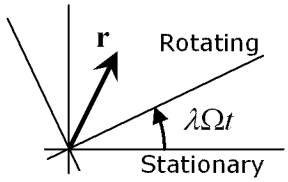

Fig.12: Average fluid velocity

given by the formulas

$$\begin{aligned} \mathbf{r}_{\mathrm{rot}} &= \mathbf{r}\, \exp(-\mathrm{j}\,\lambda\,\Omega\,t)\ , \\ \dot{\mathbf{r}}_{\mathrm{rot}} &= (\dot{\mathbf{r}} - \mathrm{j}\,\lambda\,\Omega\,\mathbf{r})\, \exp(-\mathrm{j}\,\lambda\,\Omega\,t)\ . \end{aligned} \tag{2}$$

Substitution into the fluid force equation results in the following formula

$$\mathbf{F} = K\,\mathbf{r} + D\,\dot{\mathbf{r}} - \mathrm{j}\,D\,\lambda\,\Omega\,\mathbf{r}\ , \tag{3}$$

where the complex term $\mathrm{j}\,D\,\lambda\,\Omega\,\mathbf{r}$ has the meaning of the force acting in the perpendicular direction to the vector $\mathbf{r}$ and this force is called tangential. As the rotor angular velocity increases, this force can become very strong and can cause instability of the rotor behavior.

As it was mentioned the rotor is under influence of the external forces, for instance produced by unbalance mass or simply by gravity. This external perturbation force is assumed to be rotating at the angular velocity ω, which is considered to be completely independent on the rotor angular velocity Ω to obtain general solution [4, 5]. The unbalance force, which is produced by unbalance mass m mounted at a radius r_{u} and rotating at the angular velocity ω, acts in the radial direction and has a phase δ at time $t = 0$

$$\mathbf{F}_{\mathrm{perturbation}} = m\,r_{\mathrm{u}}\,\omega^2\ \exp[\mathrm{j}(\omega\,t + \delta)]\ . \tag{4}$$

The equation of motion for a rigid rotor rotating at the steady-state rotation speed and operating in a small, localized region in the journal bearing is as follows

$$M\,\ddot{\mathbf{r}} = -K\,\mathbf{r} - D\,\dot{\mathbf{r}} + \mathrm{j}\,D\,\lambda\,\Omega\,\mathbf{r} + m\,r_{\mathrm{u}}\,\omega^2\ \exp[\mathrm{j}\,(\omega\,t + \delta)]\ , \tag{5}$$

where M is the total rotor mass. After rearranging the ordinary linear differential equation (5), the equation of motion with constant coefficients is obtained

$$M\,\ddot{\mathbf{r}} + D\,\dot{\mathbf{r}} + (K - \mathrm{j}\,D\,\lambda\,\Omega)\,\mathbf{r} = m\,r_{\mathrm{u}}\,\omega^2\ \exp[\mathrm{j}\,(\omega\,t + \delta)]\ . \tag{6}$$

The solution of this type of equation is well known. It is assumed as a response vector with magnitude $\mathbf{A}$ and phase α and rotating at the angular velocity ω

$$\mathbf{r} = \mathbf{A}\ \exp[\mathrm{j}\,(\omega\,t + \alpha)]\ , \qquad \dot{\mathbf{r}} = \mathrm{j}\,\omega\,\mathbf{A}\ \exp[\mathrm{j}\,(\omega\,t + \alpha)]\ , \qquad \ddot{\mathbf{r}} = -\omega^2\,\mathbf{A}\ \exp[\mathrm{j}\,(\omega\,t + \alpha)]\ . \tag{7}$$

The magnitude and phase of the journal centre is given by the following formula

$$\mathbf{A}\ \exp(\mathrm{j}\,\alpha) = \frac{m\,r_{\mathrm{u}}\,\omega^2\ \exp(\mathrm{j}\,\delta)}{(K - M\,\omega^2) + \mathrm{j}\,D\,(\omega - \lambda\,\Omega)}\ . \tag{8}$$

Let the unbalance force excitation frequency is the same as the rotor angular velocity $\omega = \Omega$ for the experimental data. Then the general non-synchronous model is converted to the special synchronous model

$$\mathbf{A}\ \exp(\mathrm{j}\,\alpha) = \frac{m\,r_{\mathrm{u}}\,\Omega^2\ \exp(\mathrm{j}\,\delta)}{(K - M\,\Omega^2) + \mathrm{j}\,D\,\Omega\,(1 - \lambda)}\ . \tag{9}$$

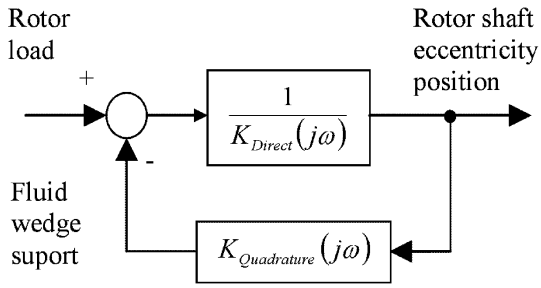

Fig.13: Transform to stationary coordinates

This solution (9) describes the rotor motion, which is shown in figure 8, with the relatively small amplitude. The frequency of the dominating component in the frequency spectra for the part of the signal record without self-exciting vibration is equal to the rotor rotational frequency.

The rotor/fluid wedge bearing/system can be demonstrated as a servomechanism working in the closed loop, which is shown in figure 13. The direct and quadrature dynamic stiffness is introduced according to the acting force direction. To obtain the Laplace transform of the mentioned dynamic stiffness, the imaginary variable $\mathrm{j}\,\omega$ is replaced by a complex variable s

$$K_{\mathrm{direct}}(s) = K + D\,s + M\,s^2\ , \qquad K_{\mathrm{quadrature}}(s) = -\mathrm{j}\,\lambda\,\Omega\,D \tag{10}$$

and the journal centre displacement can be evaluated in the form

$$\mathbf{r} = \frac{\mathbf{F}_{\mathrm{perturbation}} - K_{\mathrm{quadrature}}(s)\,\mathbf{r}}{K_{\mathrm{direct}}(s)}\ . \tag{11}$$

The individual transfer function $1/K_{\mathrm{direct}}(s)$ (direct dynamic compliance) is stable. The feedback path in the closed-loop system acts as a positive feedback and introduces instability for the closed-loop system. The gain of the positive feedback depends on the angular velocity Ω. The closed-loop system is stable for the low rotor rotational speed. There is a margin for the stable behavior. If the gain of the positive feedback crosses over a limit value then the closed-loop becomes unstable. The properties of the unstable behavior can be analyzed using the servomechanism in figure 13.

The stability of the closed-loop dynamic system is depending on the open-loop frequency transfer function for

$$G_0(\mathrm{j}\,\omega) = \frac{K_{\mathrm{quadrature}}(\mathrm{j}\,\omega)}{K_{\mathrm{direct}}(\mathrm{j}\,\omega)} = \frac{-\lambda\,\Omega\,D}{\omega\,D - \mathrm{j}\,(K - M\,\omega^2)}\ . \tag{12}$$

As it is known the closed-loop dynamic system is stable according to the Nyquist stability criterion if, and only if, the locus of the $G_0(\mathrm{j}\,\omega)$ function in the complex plane does not enclose the $(-1, 0)$ point as ω is varied from zero to infinity [10]. Enclosing the $(-1, 0)$ point is interpreted as passing to the left of the mentioned point. The $G_0(\mathrm{j}\,\omega)$ locus for three different values of the rotor angular velocity Ω is shown in Nyquist diagram in figure 14, which is ploted as an ilustrating example for $K/D = 100\,\mathrm{rad/s}$. All the contour plots are of the same shape. They are differing only in a scale and correspond to the stable, steady-state and unstable vibration. When the steady-state vibration occurs, the stability margin

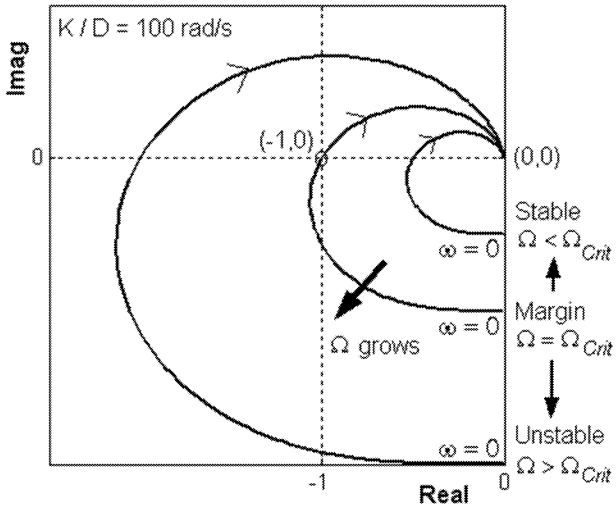

Fig.14: Shaft/fluid wedge bearing/system as a servomechanism

is achieved. The locus of the $G_0(\mathrm{j}\,\omega)$ function, describing the steady-state vibration, meets the $(-1, 0)$ point, therefore

$$G_0(\mathrm{j}\,\omega_{\mathrm{crit}}) = -1 \ . \tag{13}$$

An angular frequency, at which a system can oscillate without damping, is designated by ω_{crit}. Substitution (13) into (12) results in formulas for the oscillating frequency

$$\omega_{\mathrm{crit}} = \frac{K}{M} \qquad \text{and} \qquad \omega_{\mathrm{crit}} = \lambda\,\Omega \ . \tag{14}$$

It can be concluded that the frequency of the rotor subharmonic oscillation is the same as the fluid average angular velocity. The measurement shows that the value of the parameter λ is equal to 0.475. This result confirms the introductory assumption about the fluid forces acting on the rotor. The stability margin corresponds to the mechanical resonances of the rigid rotor mass supported by the oil spring. It can be noted that the frequency ω_{crit} is not equal to the rotor critical speed when the vibration is excited by the rotor unbalance.

If the system were linear, then the unstable rotor vibration would spiral out to infinity when the rotor angular frequency crosses the so-called Bently-Muszynska threshold

$$\Omega_{\mathrm{crit}} = \frac{\sqrt{\dfrac{K}{M}}}{\lambda} \ . \tag{15}$$

The Bently-Muszinska threshold is inversely proportional to the ratio λ. The anti-swirl technique is focused at decreasing λ.

As it is experimentally verified, the frequency spectrum of the fluid induced oscillation contains the single dominating component as it would be a solution of the second order linear differential equation without damping. The proportionality between ω and Ω is maintained for a wide range of Ω, which is greater than the threshold Ω_{crit}. This fact is confirmed by the full multispectrum in figure 11. The dominating peak in all the spectra forms a straight line in the waterfall plot. Therefore the multispectrum can be considered as an experimental

verification of the fact that the value of λ is constant and independent on the rotor rotational speed.

The journal lateral oscillations are limited by the journal bearing surface. Stiffness and damping coefficients are non-linear functions of the eccentricity ratio, especially when the journal is approaching to the bearing wall. If the magnitude of vibration is increasing then the fluid-film stiffness and damping is increasing as well and the relationship (14) is maintained adapting stiffness to the value of $M\,\omega^2$. A new balance forms a limit cycle of the journal orbital motion.

A fluid-induced instability, commonly referred to as oil whirl, is the special resonance vibration with the frequency that is proportional to the journal rotational speed. The rotor precession is self-excited by fluid induced instability and it is called whirl vibration. The whirl vibration is always forward precession and starts at the rotor rotational frequency given by (15). The orbit shape is nearly circular for whirl vibration [7].

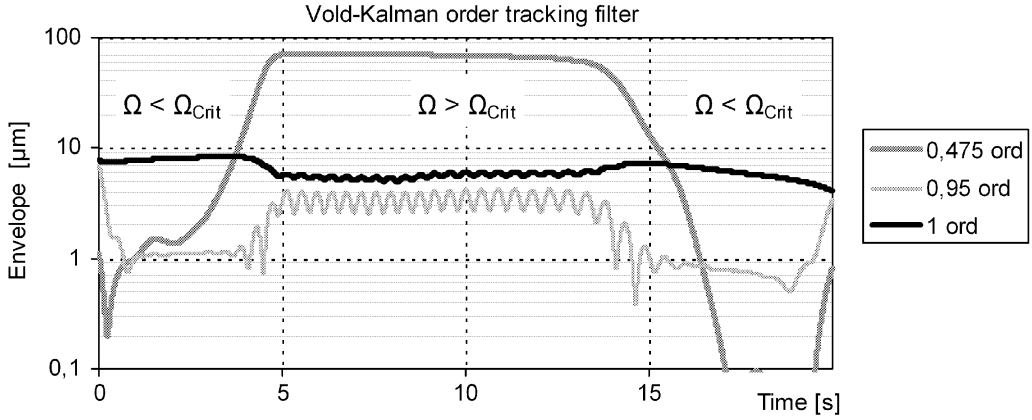

Fig.15: Nyquist diagram showing stable, margin and unstable locus

5. Magnitude of the whirl vibrations

The magnitude of the whirl vibration at the frequency $\lambda\,\Omega$ (0.475 ord), including the second harmonic (0.95 ord) of this frequency, and the magnitude of the vibration at the rotor rotational frequency Ω (1 ord) as a function of time are shown in figure 15. The frequencies of the tracked components are designated by order, which is a fraction or multiple of the rotor rotational frequency. The magnitudes as harmonic vibration envelopes were evaluated using the Vold-Kalman order tracking filtration [11]. As it follows from the formula (9), the magnitude of the synchronous component is proportional to the inverse term, which depends on the value of the oil-film stiffness. The diagram in figure 15 shows that the magnitude is decreasing while the self-excited vibration starts as a result of the stiffness increase. The same effect can be seen, when the self-excited vibration stops. This phenomenon confirms the hypothesis stated for explanation why the steady-state vibration is maintained for $\Omega > \Omega_{\mathrm{crit}}$.

The magnitude of the 0.475 ord component is ten times greater at least than the magnitude of its second harmonic (0.95 ord). The presence of the harmonics is a correctness measure for assumption dealing with linearity of the rotor system.

The magnitude of the vibration at the journal vibration frequency ($\lambda\,\Omega$) as a function of the rotor rotational frequency (Ω) is shown in figure 16. The segment AB of the diagram

corresponds to the RPM interval where the whirl vibration occurs and the oil film stiffness is adapted to save equality of the quantities $M\,\omega^2$ and K while $\omega = \lambda\,\Omega$. The magnitude of the whirl steady-state vibration depends slightly on the rotor RPM. The formula (8) theoretically gives the infinity magnitude for these conditions. As it is evident the thresholds for starting and stopping the fluid-induced vibration are different, which is a consequence of the rotor system non- linearity. Stiffness and damping of the oil-film for real rotor systems are not only a function of the vibration magnitude but a function of Ω as well. Except for some experimental result the analytical solution is beyond the topic of this paper.

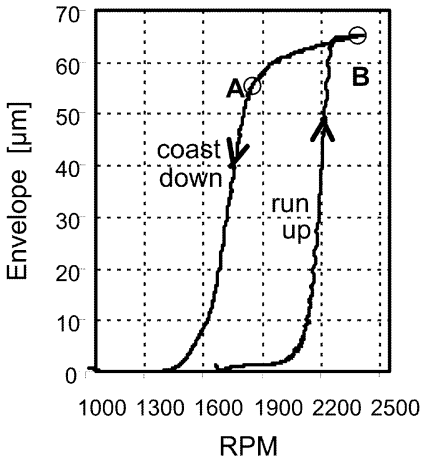

Fig.16: Envelope of the vibration at the frequency $\lambda\,\Omega$ versus shaft RPM

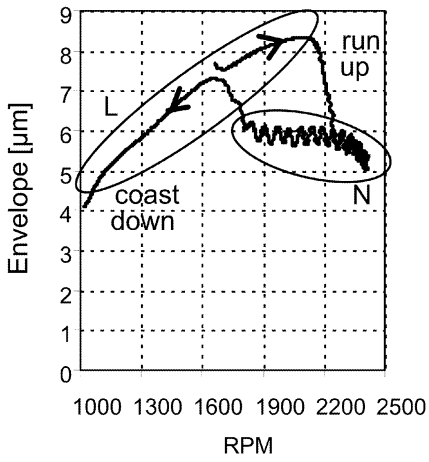

Fig.17: Envelope of the vibration at the frequency Ω versus shaft RPM

The magnitude of the vibration at the rotor rotational frequency (Ω) as a function of this frequency (Ω) is shown in figure 17. This diagram indicates that there are two states of the rotor system. The state of the damped vibration is described by the linear motion equation (6) with constant parameters while the fluid-induced vibration can be described by the same equation but some of the parameters, namely stiffness and damping, are a function of the vibration magnitude.

During the rotor run up and coast down the magnitude of the synchronous spectrum component is free of extreme resonances what confirms that the maximum value of the rotation speed is less than the first critical speed. Some experiments [7] show that the self-excited vibration at the frequency $\lambda\,\Omega$ stops when passing the first rotor critical speed. If the rotational speed of the Rotor Kit exceeds thousands of RPM the whip vibration appears. The frequency of the whip oscillation is equal to a constant value.

6. Conclusion

The paper describes a powerful analytical tool for rotor system diagnostics. The new term is a full spectrum. The full spectrum is a good tool for stability investigation of rotors supported by fluid film bearings. An advantage of the full spectrum is that this two- side spectrum describes motion in the plane while the one-side spectrum describes motion along a straight line. The two-side spectrum allows evaluating the orbit envelope. The first part of the paper demonstrates whirl vibration and the independence of the ratio relating the precession speed to the rotor rotational speed on the rotor absolute rotational speed.

The lumped parameter model of the journal centre motion in the journal bearing gives explanation of the stability margin and the onset of the self-excited vibration. The analysis of the journal behavior is based on using the Nyquist stability criterion for linear dynamic systems. The Vold-Kalman filter, employed to track the harmonics of the rotor rotational frequency, gives the new and interesting information about the rotor system properties. As it is evident the journal motion in bearing is governed by two equations of motion, the first one for a small amplitude of vibration (linear model) and the second one for the fluid-induced vibration (non- linear model).

Acknowledgement

This research has been supported by the Czech Grant Agency as a part of the project No. 101/07/1345.

References

[1] Joh Y.D., Lee C.-W.: Korea Advanced Institute of Science, Taejon, South Korea, Excitation Methods and Modal Parameter Identification in Complex Modal Testing of Rotating Machinery. Modal Analysis: the International Juurnal of Analytical and Experimental Modal Analysis, Vol. 8, N. 3, July 1993, p. 179–203
[2] Qu L.: Rotating Machinery Fault Diagnosis Using Wigner Distribution, Academic Press Limited, 1991
[3] Tondl A.: Some Problems of Rotor Dynamics, Publishing House of the Czechoslovak Academy of Sciences, Prague 1965
[4] Muszynska A.: Whirl and Whip – Rotor / Bearing Stability Problems, Journal of Sound and Vibration (1986) 110 (3), pp. 443–462
[5] Bently D.E., Muszynska A.: Fluid-generated Instabilities of Rotors, Orbit, Volume 10, No. I, April, 1989
[6] Ecker H., Tondl A.: Increasing the Stability Threshold of a Rotor by Open-Loop Control of the Bearing Mount Stiffness, In: Proceedings of ISCORMA-3, Cleveland, Ohio, 19–23 September 2005
[7] Bently D.E., Muszynska A.: Role of Circumferential Flow in the Stability of Fluid-Handling Machine Rotors, The Fifth Workshop on Rotordynamics Instability Problems in High Performance Turbomachinery, Texas A&M University, College Station, Texas, 16-IR May 1988, pp. 415–430
[8] Tondl A.: Quenching of self-excited vibrations, Academia, Prague 1991
[9] Flack R.D., Kostrzewsky G.J., Barrett L.E.: Experimental and predicted rigid rotor stability threshold of axial groove and three-lobe bearing, International Journal of Rotating Machinery, 8 (1), 27–33, 2002
[10] Burns R.: Advanced control Engineering, Butterworth Heinemann, Oxford 2001
[11] Tůma J.: Setting the passband width in the Vold-Kalman order tracking filter, In: 12th International Congress on Sound and Vibration, (ICSV12), Lisabon, July 11–14, 2005, Paper 719

Received in editor's office: March 16, 2006
Approved for publishing: November 2, 2006

Note: The paper is an extended version of the contribution presented at the national colloquium with international participation *Dynamics of Machines 2006, IT AS CR, Prague, 2006.*